Finite Element Analysis of Homogeneous Waveguide Modes

Alex D. Santiago-Vargas
Electrical and Computer Engineering
Purdue University
West Lafayette, IN
adsv@purdue.edu

***Abstract*—Waveguides are common high power and low-loss microwave transmission lines. Simple geometries like rectangular and circular crossections of homogeneous media have well known analytical solutions. For arbitrary geometries, finite element method can be used to analyze the propagation modes and cutoff frequencies numerically. The method fits arbitrary geometry well as the mesh discretization can conform to curved edges. This paper presents the implementation of the finite element method for the analysis of homogeneously-filled waveguides. Rectangular, ridge, circular, and coaxial crossections are analyzed up to the fourth propagation mode.**

***Index Terms*—Finite Element Method, Homogeneous Waveguides**

I. Introduction

In high-power RF and microwave engineering, the loss between components should be minimized. Waveguides provide low propagation loss and high power handling at high frequencies. They are also electrically isolated, as the boundary shields the signal from interference. Compared to a two-conductor transmission line like a coaxial cable, the waveguide can only propagate Transverse Electric (TE) or Transverse Magnetic (TM) modes. Coaxial lines can support the propagation of true Transverse Electromagnetic (TEM) modes.

The analytical solutions for simple geometries like rectangular or circular crosssections are well known. For example, in a rectangular waveguide, the cutoff frequencies are given by

$$f_{c,mn} = \frac{k_c}{2\pi\sqrt{\mu\varepsilon}} = \frac{1}{2\pi\sqrt{\mu\varepsilon}}\sqrt{\left(\frac{m\pi}{a}\right)^2 + \left(\frac{n\pi}{b}\right)^2} \qquad (1)$$

where a and b are the dimensions of the waveguide, $m, n = 0, 1, 2, ...$, but m and n cannot be zero simultaneously [1].

The Finite Element Method (FEM) breaks down the problem with an arbitrary geometry, for example a triangle, in a process known as meshing. Each node and element are labeled with a unique number. Fig. 1 shows the mesh for an arbitrary shape. A linear eigenvalue equation is derived from the partial differential equations (PDE) boundary value problem (BVP) to solve the equations. Following Galerkin's method for weighted residuals, each element contributes to the global problem matrices with weighting and interpolating functions (i.e., linear, quadratic, etc. interpolation) to construct the eigenvalue problem. Each local node is numbered similarly, but they contribute to the corresponding global node as shown in Fig. 2.

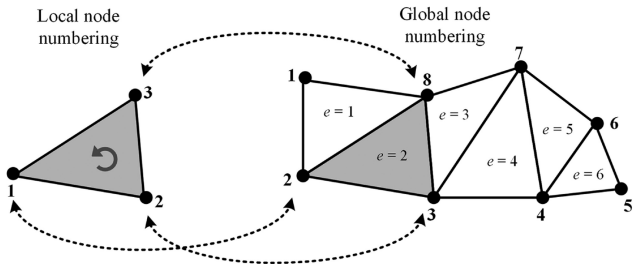

Fig. 1: Finite Elements. Taken from [2].

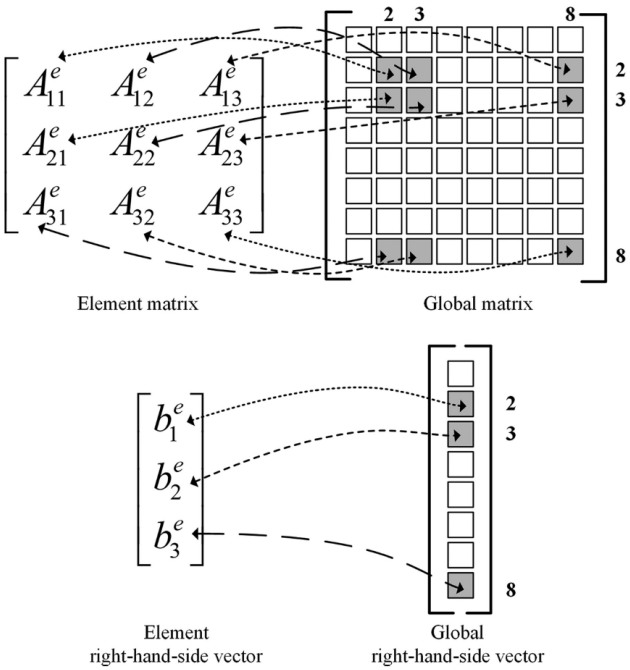

Fig. 2: FEM Matrix Assembly. Taken from [2].

This paper is divided as follows: Section II-A presents the derivation for the FEM applied to the propagation modes on an homogeneously filled arbitrarily shaped waveguide. Section II-B explains the meshing process that was used in this paper. Section III shows the resulting field distributions and dispersion curves for rectangular, ridge, circular, and coaxial waveguides. Section IV summarizes results and concludes.

II. Method Formulation

A. Mathematical Formulation

Waveguide structures with uniform cross-sections can be analyzed in a reduced 2D domain to determine each propagation mode's cutoff frequency and field intensities. The cross-section can have any arbitrary shape, given that it is constant along the propagation direction. The analysis of the problem is divided into two cases. The first case is the Transverse Electric (TE) mode, where the electric field has no component in the direction of propagation. The second case is the Transverse Magnetic (TM) mode, where the magnetic field has no component in the propagation direction. In both TE and TM modes, the electric and magnetic fields, respectively, only exist in the 2D crosssection transverse to the propagation direction. The following derivation assumes a waveguide oriented in the $\hat{z}$ direction, with a perfect electric conductor (PEC) boundary and homogeneous media (constant permittivity and permeability in the structure). A propagating wave in the waveguide will take the form

$$\mathbf{E}(\mathbf{x},\mathbf{y},\mathbf{z}) = \big[\mathbf{E_t}(\mathbf{x},\mathbf{y}) + \hat{z}E_z(x,y)\big]e^{-\gamma z} \tag{2}$$

$$\mathbf{H}(\mathbf{x},\mathbf{y},\mathbf{z}) = \big[\mathbf{H_t}(\mathbf{x},\mathbf{y}) + \hat{z}H_z(x,y)\big]e^{-\gamma z} \tag{3}$$

where $\mathbf{E}_t(x,y)$ is the transverse component and $E_z(x,y)$ is the longitudinal component. The propagation constant γ is defined as

$$\gamma = \alpha + j\beta. \tag{4}$$

The source-free Helmholtz wave equation can be used to study the propagation modes that can exist within the waveguide. The derivation from the source-free Maxwell's equations can be found in literature [3, Chapter 2.1.2]. The equation is defined as

$$\nabla^2\mathbf{E}(x,y,z) + k_c^2\mathbf{E}(x,y,z) = 0. \tag{5}$$

The Laplacian vector operator ∇^2 on a vector field F denotes

$$\nabla^2\mathbf{F} = \partial_x^2\mathbf{F} + \partial_y^2\mathbf{F} + \partial_z^2\mathbf{F}, \tag{6}$$

and k_c^2 is the cutoff wavenumber defined by

$$k_c^2 = k^2 - \beta^2, \tag{7}$$

with wavenumber $k^2 = \omega^2\mu\varepsilon$. The dispersion relation can be attained by rearranging Eq. (7) for β.

$$\beta = k^2 - k_c^2 \tag{8}$$

Given that the wave will propagate when β is not purely imaginary, $k^2 > k_c^2$. The input wavenumber k must be above the mode cutoff wavenumber k_c to achieve propagation instead of an evanescent wave.

For TM mode, the longitudinal component H_z will become zero with E in the $\hat{z}$ direction. The Helmholtz equation can be rewritten in terms of the transversal components only as

$$\nabla_t^2 E_z(x,y) + k_c^2 E_z(x,y) = 0 \quad \text{on } \Omega \tag{9}$$

where Ω is the solution domain and ∇_t^2 is the transversal Laplacian operator

$$\nabla_t^2\mathbf{F} = \partial_x^2\mathbf{F} + \partial_y^2\mathbf{F}. \tag{10}$$

As the boundary Γ is PEC, the Dirichlet boundary condition will be

$$E_z = 0 \text{ on } \Gamma. \tag{11}$$

By the duality principle, the equivalent source-free Helmholtz equation for TE mode ($E_z = 0$) is

$$\nabla_t^2 H_z(x,y) + k_c^2 H_z(x,y) = 0 \quad \text{on } \Omega \tag{12}$$

and the equivalent Neumann boundary condition is

$$\partial_n H_z = 0 \quad \text{on } \Gamma \tag{13}$$

where ∂_n denotes the normal derivative.

From Eqs. (9) and (12), the quantities to solve the linear system are the eigenvalue k_c^2 and the corresponding eigenvector E_z or H_z. The weak-form representation with weighting function w_i is

$$\int_\Omega \nabla_t \cdot w_i \cdot \nabla_t E_z \, d\Omega = k_c^2 \int_\Omega w_i E_z \, d\Omega + \oint_\Gamma \hat{n} \cdot (w_i E_z) \, d\Gamma \tag{14}$$

For the TM case, the boundary condition in Eq. (11) will result in the integral over the boundary becoming zero. The weak-form representation for the boundary value problem in Eqs. (9) and (11) is

$$\int_\Omega \nabla_t \cdot w_i \cdot \nabla_t E_z \, d\Omega = k_c^2 \int_\Omega w_i E_z \, d\Omega. \tag{15}$$

Let the weighting function $w_i = N_i$, where N_i is the interpolation function associated with the field value at the node $i = 1, 2, ..., N$ and N is the total number of nodes. Following Galerkin's method for weighted residuals, Eq. (15) becomes

$$\sum_{j=1}^{N} E_{z,j} \int_\Omega \nabla_t N_i \cdot \nabla_t N j \, d\Omega = k_c^2 \int_\Omega N_i N_j \, d\Omega. \tag{16}$$

Which can be written compactly as

$$[A]E_z = k_c^2[B]E_z, \tag{17}$$

where the elements A_{ij} and B_{ij} of the $[A]$ and $[B]$ matrices are defined as

$$A_{ij} = \int_{\Omega} \nabla_t N_i \cdot \nabla_t N_j \, d\Omega, \quad i,j = 1,2,...,N \tag{18}$$

$$B_{ij} = \int_{\Omega} N_i \cdot N_j \, d\Omega, \quad i,j = 1,2,...,N. \tag{19}$$

A similar process can be followed to derive the TM mode weak-form representation and solution using Galerkin's method [3]. Note the boundary condition changes to Eq. (13), which involves a different treatment to the boundary integral in the weak form. The eigenvalue and eigenvector solution to the linear system can be found with standard or sparse matrix eigenvalue numerical solver packages.

The interpolation functions for a 2D triangular element with three nodes can be written in terms of the potential as

$$\varphi^{(e)}(x,y) = a + bx + cy. \tag{20}$$

The superscript (e) denotes a value for a single element, which can be considered a local value. Each node has a potential value $\varphi_i^{(e)}$, resulting in a system of equations with the form

$$\varphi_i^{(e)} = a + bx_i^{(e)} + cy_i^{(e)}, \quad i = 1,2,3. \tag{21}$$

By solving the system of equations, the following equation is found

$$\varphi^{(e)}(x,y) = \sum_{i=1}^{3} N_i^{(e)}(x,y)\varphi_i^{(e)} \tag{22}$$

with a triangular interpolating function defined as

$$N_l^{(e)}(x,y) = \frac{1}{2\Delta^{(e)}}\left(a_l^{(e)} + b_l^{(e)}x + c_l^{(e)}y\right). \tag{23}$$

$Delta$ is the surface area for the given element calculated as

$$\Delta^{(e)} = \frac{1}{2}\left(b_1^{(e)}c_2^{(e)} - b_2^{(e)}c_1^{(e)}\right) \tag{24}$$

and the coefficients are defined as

$$a_1^{(e)} = x_2^{(e)}y_3^{(e)} - x_3^{(e)}y_2^{(e)} \tag{25}$$
$$a_2^{(e)} = x_3^{(e)}y_1^{(e)} - x_1^{(e)}y_3^{(e)} \tag{26}$$
$$a_3^{(e)} = x_1^{(e)}y_2^{(e)} - x_2^{(e)}y_1^{(e)} \tag{27}$$

$$b_1^{(e)} = y_2^{(e)} - y_3^{(e)} \tag{28}$$
$$b_2^{(e)} = y_3^{(e)} - y_1^{(e)} \tag{29}$$
$$b_3^{(e)} = y_1^{(e)} - y_2^{(e)} \tag{30}$$

$$c_1^{(e)} = x_3^{(e)} - x_2^{(e)} \tag{31}$$
$$c_2^{(e)} = x_1^{(e)} - x_3^{(e)} \tag{32}$$
$$c_3^{(e)} = x_2^{(e)} - x_1^{(e)} \tag{33}$$

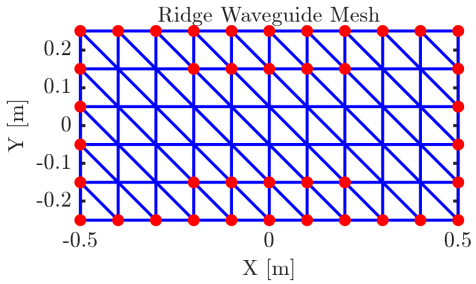

Fig. 3: Delaunay Meshing Example

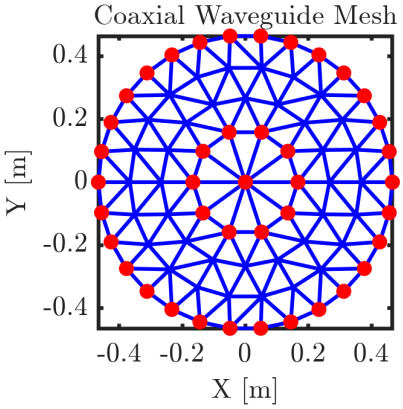

Fig. 4: Delaunay Meshing Example

B. Meshing

The geometry was meshed using MATLAB Delaunay triangulation object. Fig. 3 shows a low-resolution mesh for a Rectangular Ridge waveguide. The white triangles with blue edges are the mesh elements, the edge intersection points are the mesh nodes, and the red points are the boundary nodes. The ridge is treated as part of the boundary even though it is not at the edge of the mesh. For a rectangular waveguide, the ridge is not included in the boundary nodes. Similarly, Fig. 4 shows the mesh for a coaxial waveguide. The center conductor is included as part of the boundary nodes to achieve the same effect as on the rectangular ridge waveguide.

III. Numerical Experiments

A. Rectangular Waveguide

A rectangular waveguide with dimensions of $1m \times 0.5m$ was simulated with a discretization length of $0.001m$. The waveguide was homogeneously filled with free space with $\varepsilon = 8.85418781 \cdot 10^{-12}, \mu = 4\pi \cdot 10^{-7}$. Figs. 5 and 6 show the first four TE and TM propagation modes. When comparing the results to [1], [4], the propagation modes follow the same field intensity distributions. Figs. 5e and 6e shows the dispersion curves for the first four modes.

B. Rectangular Ridge Waveguide

By adding a conducting ridge to the rectangular waveguide with dimensions $0.5m \times 0.25m$ to the previous case, the bandwidth for the waveguide is effectively extended. Figs. 7

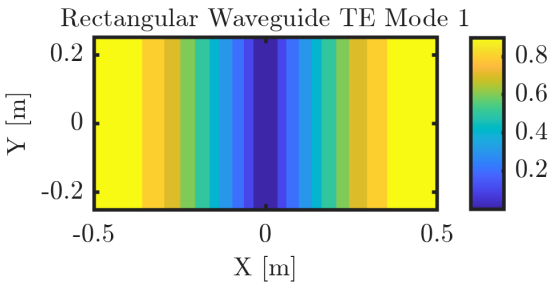

(a) TE_{10} Field Distribution

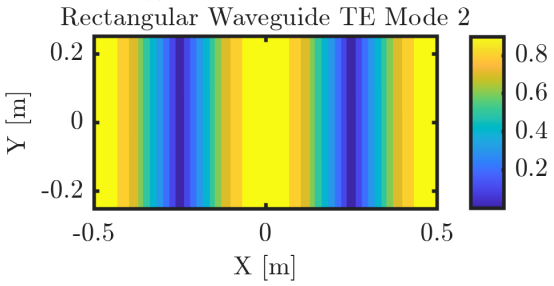

(b) TE_{20} Field Distribution

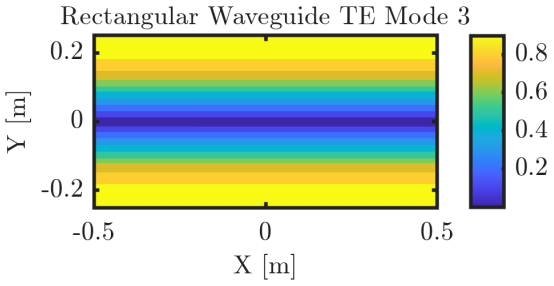

(c) TE_{01} Field Distribution

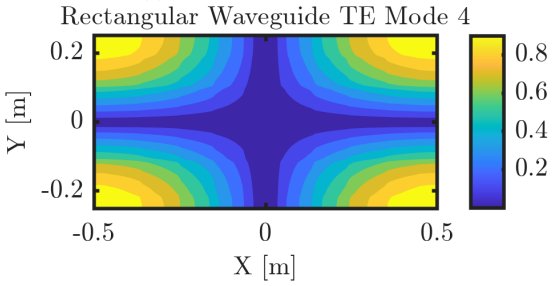

(d) TE_{11} Field Distribution

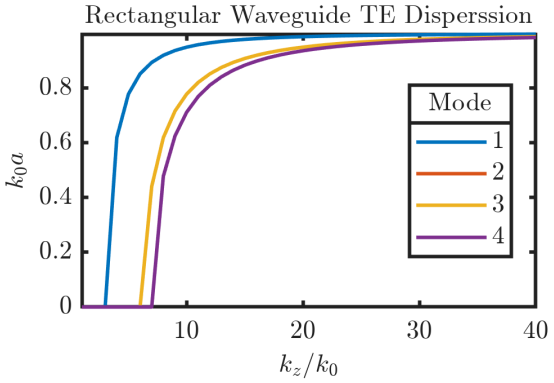

(e) Disperssion

Fig. 5: Rectangular Waveguide TE Mode

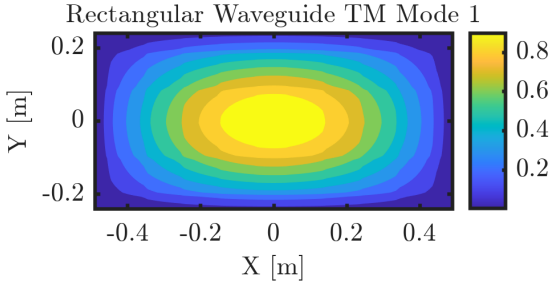

(a) TM_{11} Field Distribution

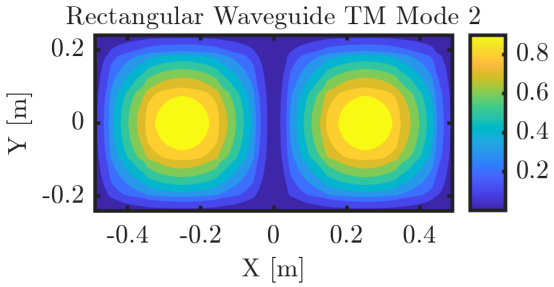

(b) TM_{21} Field Distribution

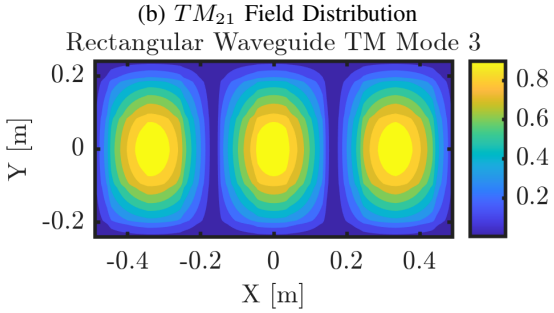

(c) TM_{31} Field Distribution

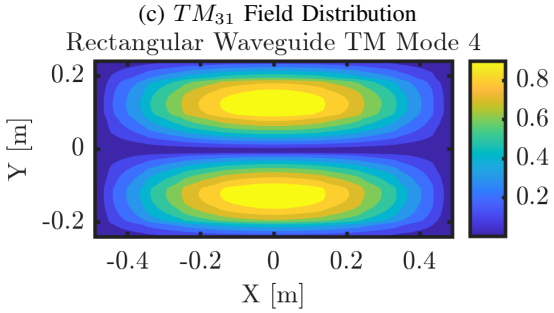

(d) TM_{12} Field Distribution

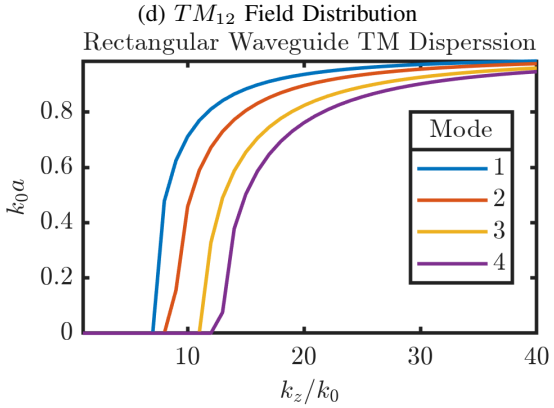

(e) Disperssion

Fig. 6: Rectangular Waveguide TM Mode

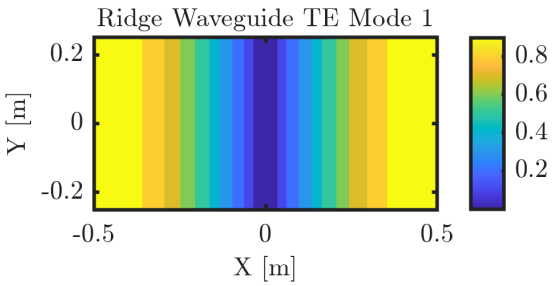

(a) TE_{10} Field Distribution

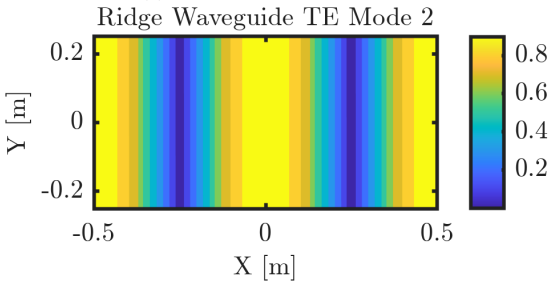

(b) TE_{20} Field Distribution

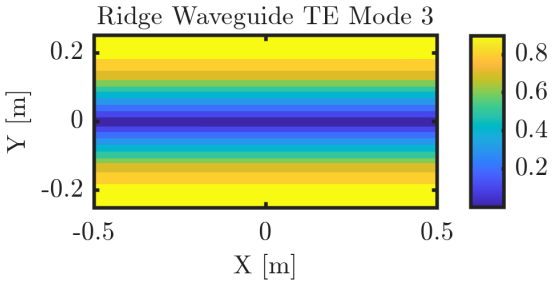

(c) TE_{01} Field Distribution

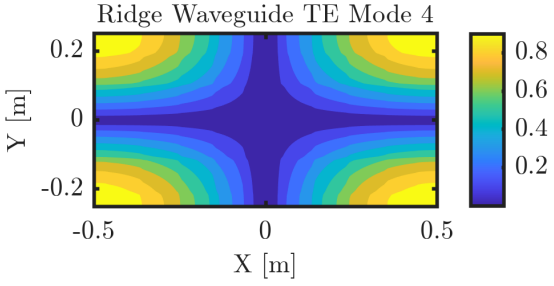

(d) TE_{11} Field Distribution

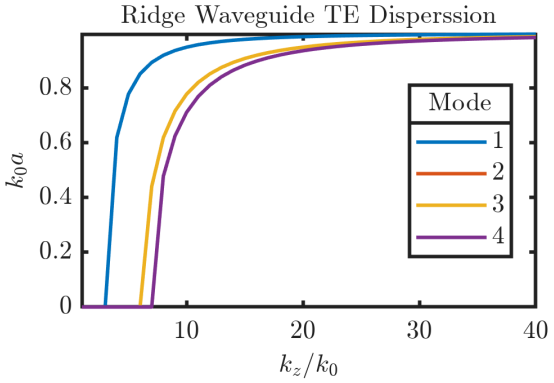

(e) Disperssion

Fig. 7: Ridge Waveguide TE Mode

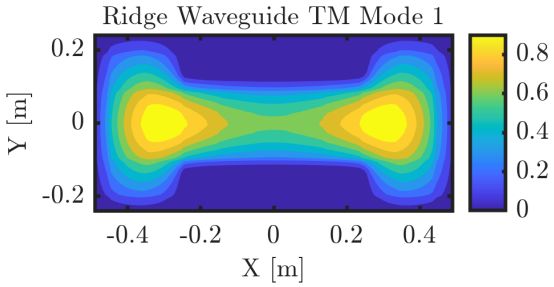

(a) TM_{11} Field Distribution

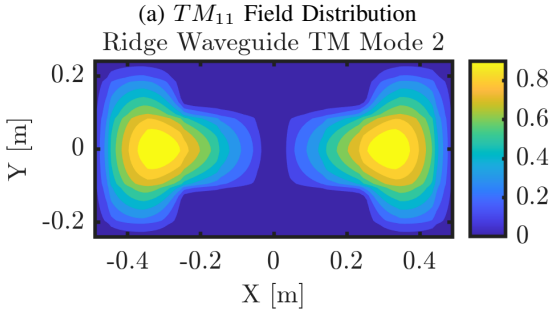

(b) TM_{21} Field Distribution

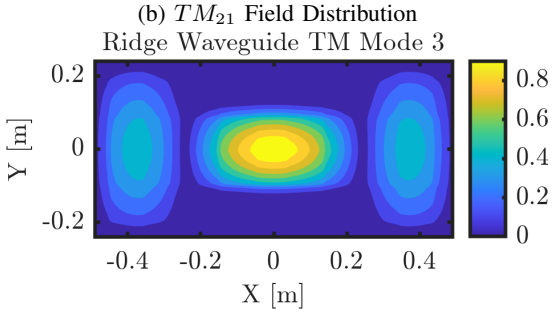

(c) TM_{31} Field Distribution

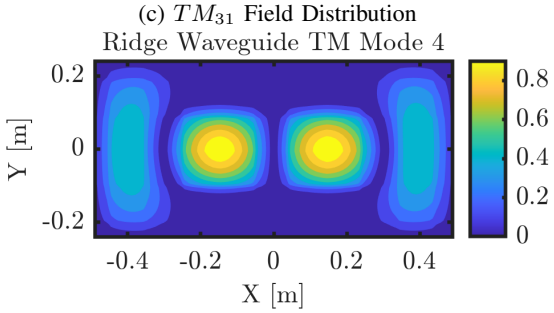

(d) TM_{41} Field Distribution

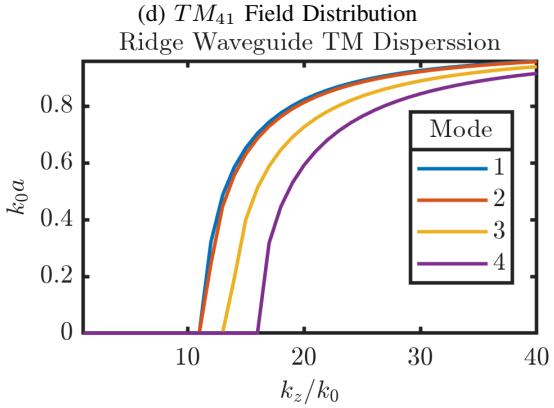

(e) Disperssion

Fig. 8: Ridge Waveguide TM Mode

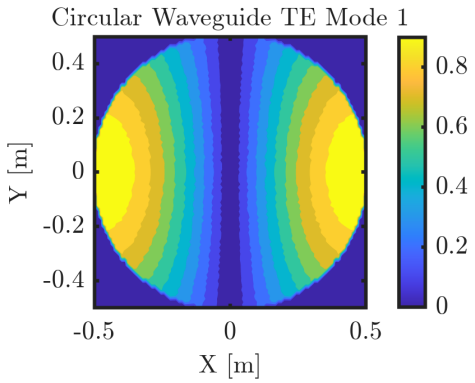

(a) TE_{10} Field Distribution

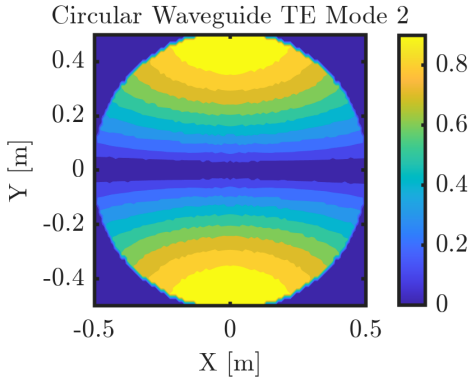

(b) TE_{01} Field Distribution

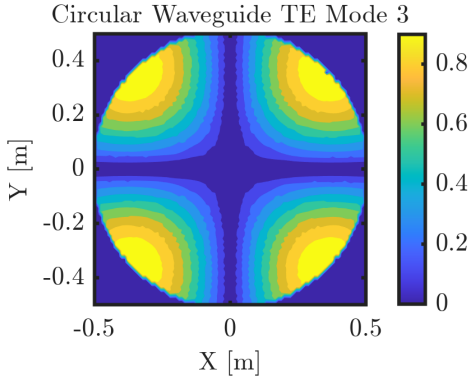

(c) TE_{11} Field Distribution

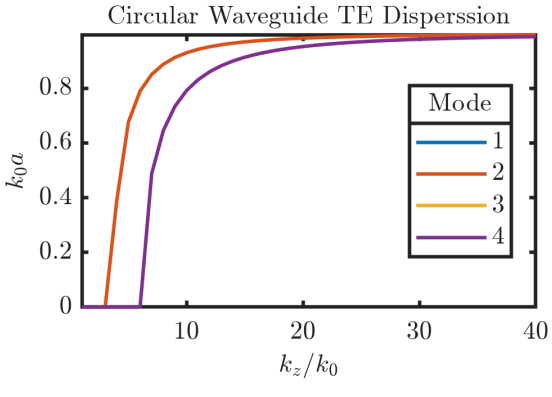

(d) Disperssion

Fig. 9: Circular Waveguide TE Mode

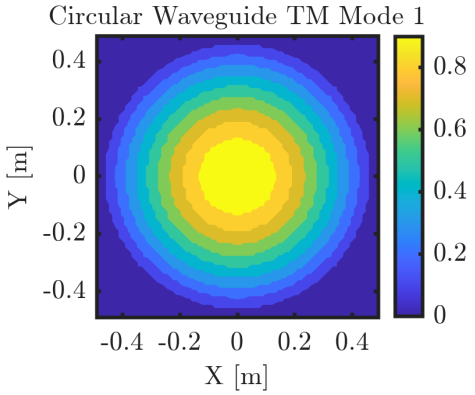

(a) TM_{11} Field Distribution

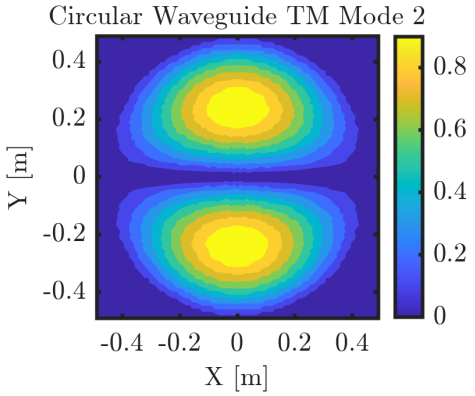

(b) TM_{12} Field Distribution

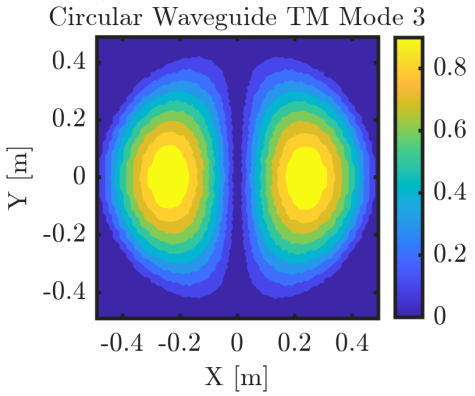

(c) TM_{21} Field Distribution

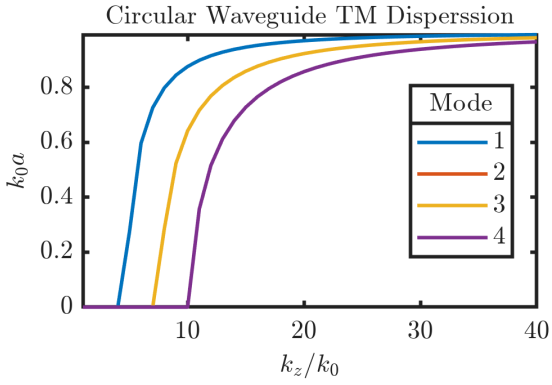

(d) Disperssion

Fig. 10: Circular Waveguide TM Mode

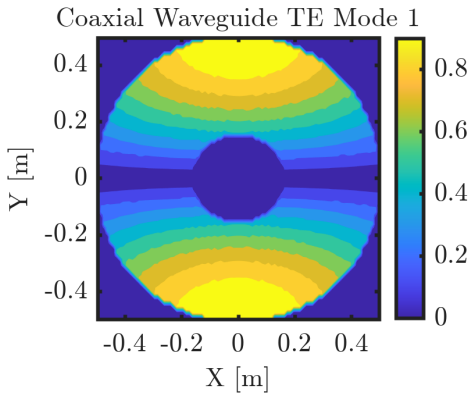

(a) TE_{01} Field Distribution

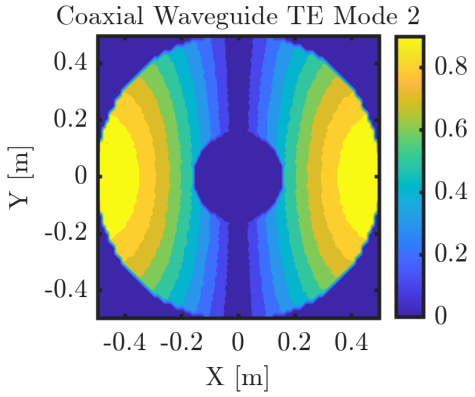

(b) TE_{10} Field Distribution

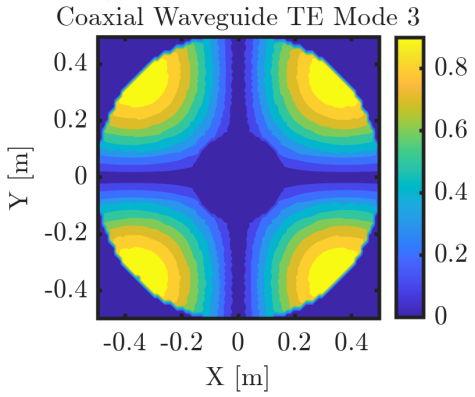

(c) TE_{11} Field Distribution

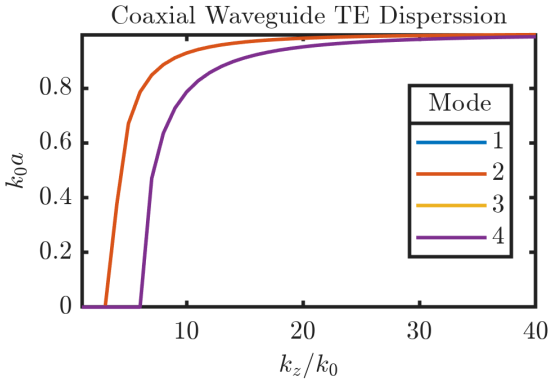

(d) Disperssion

Fig. 11: Circular Waveguide TE Mode

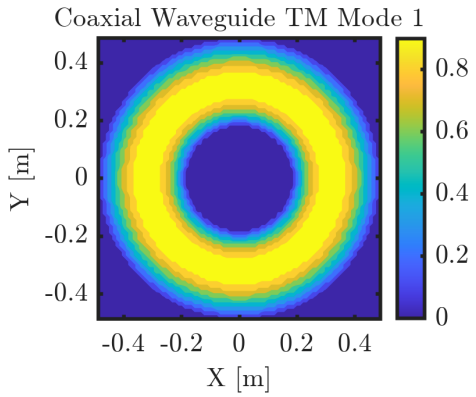

(a) TM_{11} Field Distribution

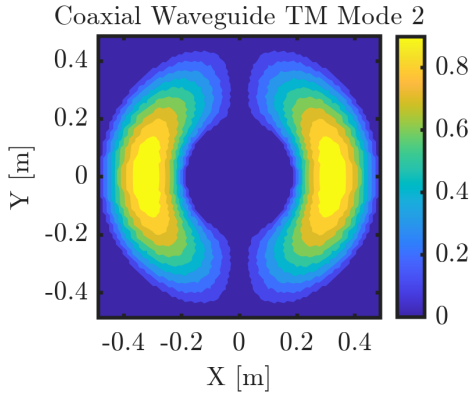

(b) TM_{21} Field Distribution

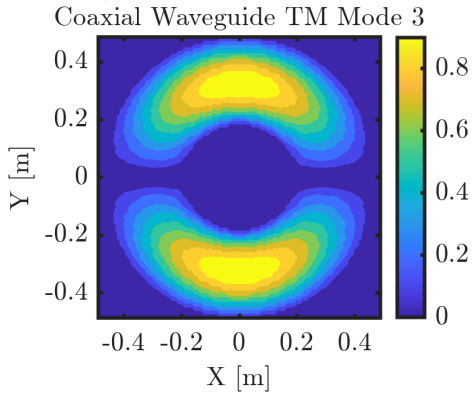

(c) TM_{12} Field Distribution

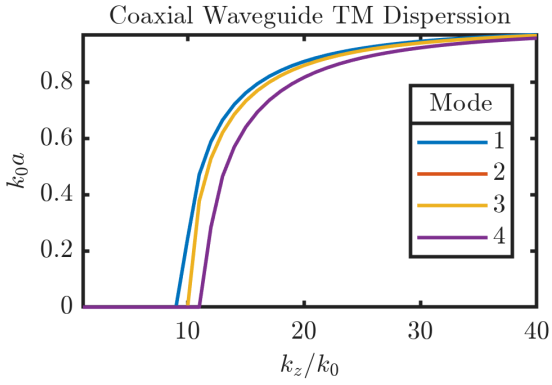

(d) Disperssion

Fig. 12: Circular Waveguide TM Mode

and 8 show the TE and TM field distributions for the first four modes. The solution will depend on the relative dimension of the ridge. The spacing between the ridge acts like a parallel plate waveguide at a higher frequency than the first mode. Its field distribution is similar to the corresponding field distributions of the rectangular waveguide in TM mode.

C. Circular Waveguide

A circular waveguide with a diameter of $1m$, discretization size of $0.001m$, and homogeneously filled free space was simulated with the same solver. Figs. 9 and 10 show the TE and TM field distributions for the first three modes. The resulting fields agree with analytical solutions that use Bessel functions ib [1] and other FEM solutions in [2].

D. Coaxial Transmission Line

The TE and TM modes propagating in a coaxial line can also be simulated by adding a center conductor with the same technique as the ridge in the rectangular waveguide. The modes for a center conductor of diameter $0.33m$ are shown in Figs. 11 and 12. Note that the fields take form of rings. Note that fields are not present in the location of the center conductor. Also, the fields are concentrated in the ring within a smaller area than the circular waveguide.

IV. Conclusion

FEM analysis allows for frequency domain simulations that avoid the staircase error from Finite Difference Time Domain (FDTD) simulations. The field intensities for TE and TM modes in rectangular, ridge, circular, and coaxial waveguides were presented and compared to existing analytical and numerical results. This method can provide a numerical solution to complex geometries that analytical solutions have not yet been found. The implementation in this paper is limited to homogeneously filled waveguides but can be extended to non-homogeneous media.

References

[1] D. M. Pozar, *Microwave Engineering*. John wiley & sons, 2011.

[2] Ö. Özgün and M. Kuzuoğlu, *MATLAB-based Finite Element Programming in Electromagnetic Modeling*. CRC Press, 2018.

[3] J.-M. Jin, *The Finite Difference Method*, pp. 295–341. Wiley-IEEE Press, 2010.

[4] M. Steer, "Microwave and rf design," 2019.